Conference paper

José V. Prata*, Patrícia D. Barata and Gennaro Pescitelli

Inherently chiral calix[4]arenes with planar chirality: two new entries to the family

Abstract: The synthesis of two new inherently chiral calix[4]arenes (ICCs, **1** and **2**), endowed with electron-rich concave surfaces, has been achieved through the desymmetrization of a lower rim distal-bridged oxacyclophane (OCP) macrocycle. The new highly emissive ICCs were resolved by chiral HPLC, and the enantiomeric nature of the isolated antipodes proved by electronic circular dichroism (CD). Using time-dependent density functional calculations of CD spectra, their absolute configurations were established. NMR studies with (*S*)-Pirkle's alcohol unequivocally showed that the host-guest interactions occur in the chiral pocket comprehending the calix-OCP *exo* cavities and the carbazole moieties.

Keywords: absolute configuration assignment; Calix[4]arenes; chiroptical properties; fluorescence; POC-2014; planar chirality; TDDFT calculations.

DOI 10.1515/pac-2014-0707

Introduction

Calixarenes are widely recognized as one of the most useful classes of synthetic molecular receptors [1, 2]. Endowed with the capability of recognizing neutral molecules, metal and molecular cations, and anions, calixarenes have been extensively used as building blocks in the construction of countless three-dimensional hosts for applications in various fields [1–3]. Calix[4]arene compounds in particular, due to their bowl-shaped intramolecular cavities in a cone conformation, are known to selectively interact with structurally complementary molecular species in fluid phase and solid state, once structural rigidification and proper functionalization of the basic calixarene skeleton has been accomplished. These two fundamental principles have been applied throughout time in the synthesis of complex calix[4]arene architectures for molecular recognition purposes. Cavitands [4, 5], calix[4]crowns [5, 6], calixspherands [7, 8], and single- and double-spanned double-cavity calixarenes [9, 10] are representative examples of this chemistry, where lower- and upper-rim bridged calix[4]arenes are produced as a means to achieve rigidification of the parent structures and thus hopefully favor their interactions with particular guests. These very same designing principles should also

Article note: A collection of invited papers based on presentations at the 15th International Conference on Polymers and Organic Chemistry (POC-2014), Timisoara, Romania, 10–13 June 2014.

***Corresponding author: José V. Prata,** Laboratório de Química Orgânica, Departamento de Engenharia Química and Centro de Investigação de Engenharia Química e Biotecnologia, Instituto Superior de Engenharia de Lisboa, Instituto Politécnico de Lisboa, R. Conselheiro Emídio Navarro, 1, 1959-007, Lisboa, Portugal, Phone: +351-218317172; Fax: +351-218317267, E-mail: jvprata@deq.isel.ipl.pt

Patrícia D. Barata: Laboratório de Química Orgânica, Departamento de Engenharia Química and Centro de Investigação de Engenharia Química e Biotecnologia, Instituto Superior de Engenharia de Lisboa, Instituto Politécnico de Lisboa, R. Conselheiro Emídio Navarro, 1, 1959-007, Lisboa, Portugal

Gennaro Pescitelli: Dipartimento di Chimica e Chimica Industriale, Università di Pisa, via Moruzzi, 3, 56124 Pisa, Italy

apply when one aims to construct useful calix[4]arene hosts for chirality-mediated processes. Having this idea in mind, we embarked in a program toward the synthesis of a new type of chiral calix[4]arenes with planar chirality, as detailed below. Envisioned applications of chiral calix[4]arenes span from enantioselective sensors, chiral selectors in chromatography separations, NMR chiral shift reagents, to enantioselective ligands in catalysis and chiral organocatalysts.

Chirality in calixarenes can be brought about in two main ways [11–13]. The simplest one is through the attachment of (at least) one chiral sub-unit of synthetic (e.g. chiral amino alcohols, epoxides, hydrocarbon chains) or of natural origin (e.g. amino acids, sugars) to the lower or upper rims of the calixarene scaffold. The second, more demanding way, explores the fact that calixarenes become chiral upon asymmetric placement of achiral sub-units on the macrocycle. These are commonly called inherently chiral calixarenes (ICCs), after Böhmer [14]. The concept of inherent chirality was lately extended to other molecular entities [15, 16]. Asymmetric substitution at the upper and/or lower rims of the macrocyclic structure (leading to AABC or ABCD substitution patterns at the aromatic rings) and single or multiple *meta*-substitution of phenolic subunits render the whole calix[4]arene asymmetric since the initial C_{4v} symmetry is broken into dissymmetric (C_2) or asymmetric (C_1) entities. These have been, by and large, the two most used routes toward ICCs [11–13].

Our strategy to ICCs differs from the above approaches, and the first example of a new class of ICCs was very recently reported by us [17]. It is based on the desymmetrization of the calix[4]arene framework upon formation of a lower rim distal-bridged oxacyclophane (OCP) macrocycle. Built up on the same approach, two new ICCs having a carbazole (CBZ) unit attached to the central phenylene ring of the OCP moiety were designed (**1** and **2**; Scheme 1). The two ICCs **1** and **2** differ by the position of CBZ attachment (position 2 or 3). Owing to the good donor abilities of *N*-alkyl CBZ derivatives, together with their usually useful fluorogenic

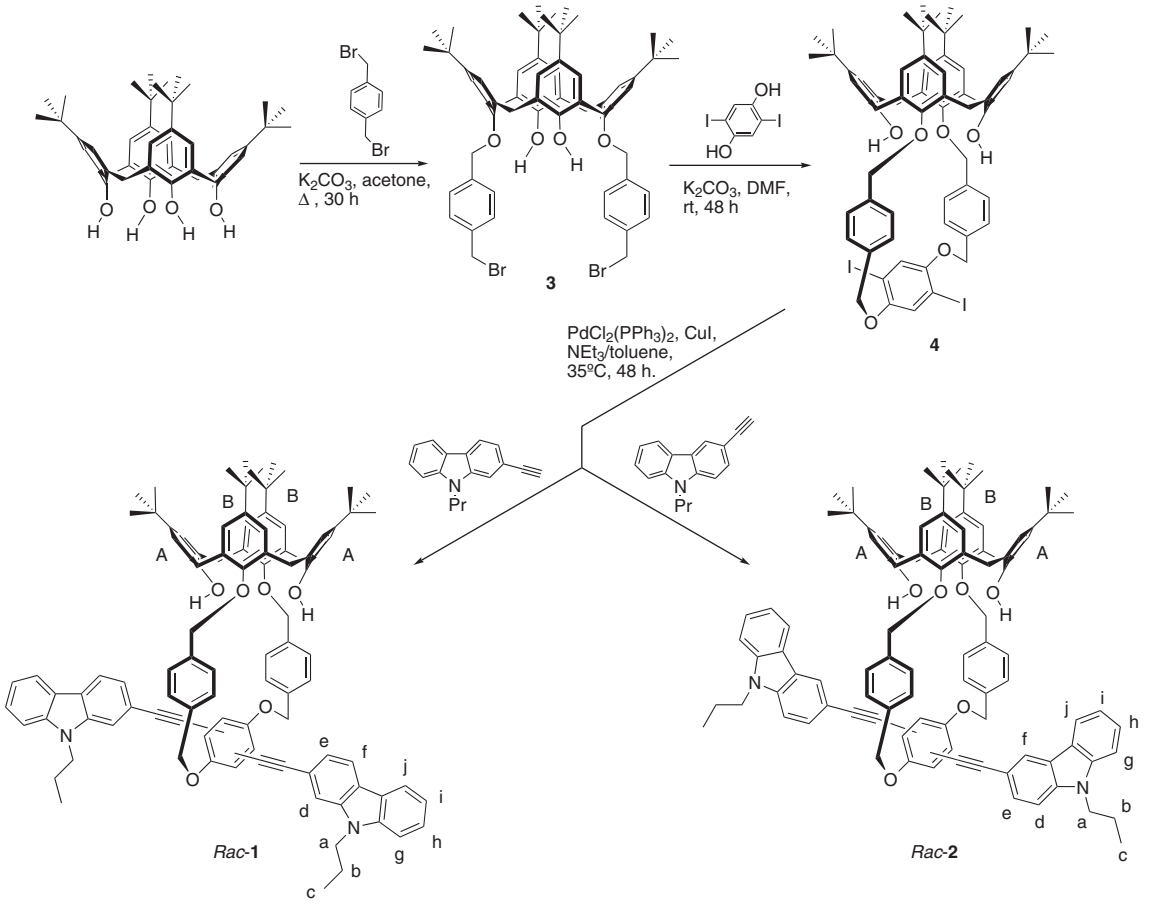

Scheme 1 Synthesis of ICCs *rac*-**1** and *rac*-**2**.

properties, it is expected that these new entries to the class of ICCs with planar chirality may find application in chiral sensing and catalysis.

Results and discussion

Synthesis and structural characterization

The synthetic route to the new ditopic molecular receptors **1** and **2** is shown in Scheme 1. By selective 1,3-(distal) etherification, the bis-bromobenzyl derivative **3** was prepared from the parent calix[4]arene and 1,4-bis(bromomethyl)benzene (K_2CO_3, acetone, reflux, 30 h) in 59 % isolated yield, by improving a previous procedure [18]. Treating **3** with 2,5-diiodohydroquinone under conditions of high dilution (K_2CO_3/DMF, rt) furnished the cyclized diiodo compound **4** [18]. The OCP derivative **4** was then double-cross coupled with 2- and 3-ethynyl-9-propyl-9*H*-carbazole, following a Sonogashira-Hagihara protocol [19], furnishing the racemic **1** and **2** in 67 % and 60 % yield, respectively, as yellow-orange solids after recrystalization from chloroform/hexane.

The new compounds **1** and **2** were characterized by spectroscopic techniques (FT-IR, $^1H/^{13}C$ NMR) and microanalysis, and full agreement with the proposed structures was found [20]. NOESY data allowed us to deduce the most stable conformations of **1** and **2** in $CHCl_3$ solution. Both compounds adopt a distorted cone conformation in the calixarene macrocycle, with the unsubstituted phenolic rings (A rings; δ_{ArH} at 7.04 and 7.03 ppm for **1** and **2**, respectively) splayed outwards and the two B rings (δ_{ArH} at 6.69 ppm) adopting a near parallel orientation between them, as depicted in Scheme 1.

This was inferred from the stronger NOE cross-peaks of aryl protons of A rings with the bridged methylene protons in equatorial positions (a pair of doublets at *ca.* 3.2 and 3.3 ppm, ArCHH_{eq}Ar) (Figs. 1 and 2). No NOE effects were observed between the arylic or phenolic protons of the calixarene A rings and those residing in

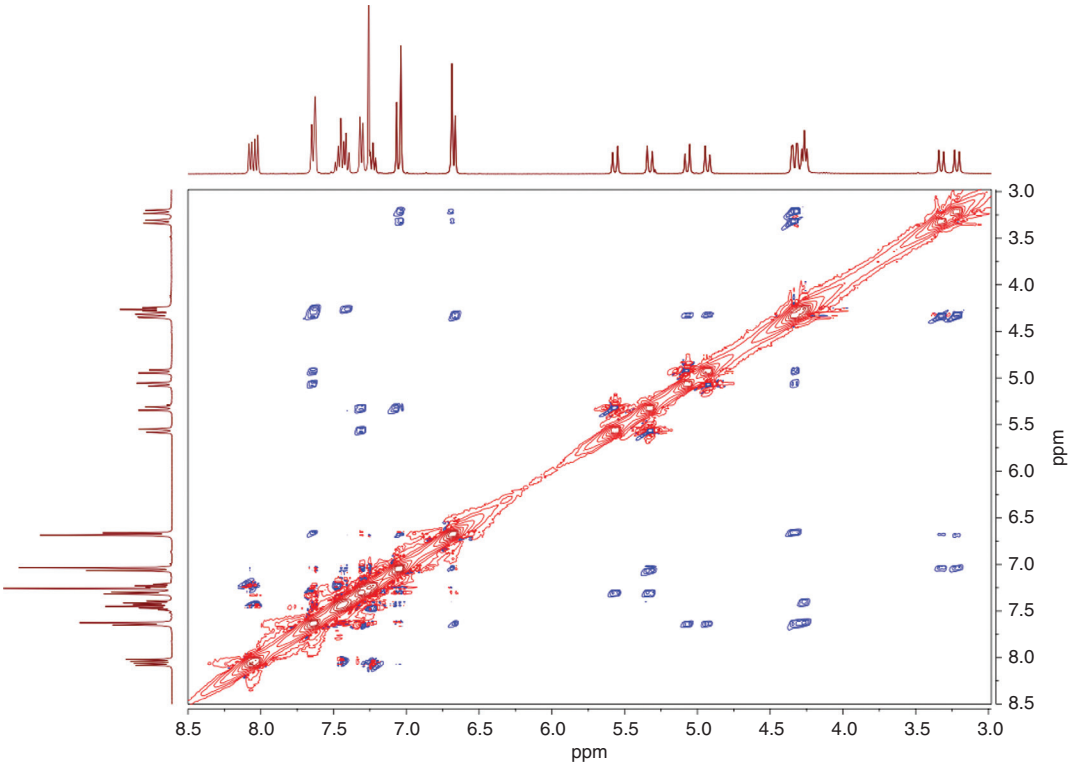

Fig. 1 NOESY spectrum (partial) of *rac*-**1** ($CDCl_3$, 400 MHz, 298 K).

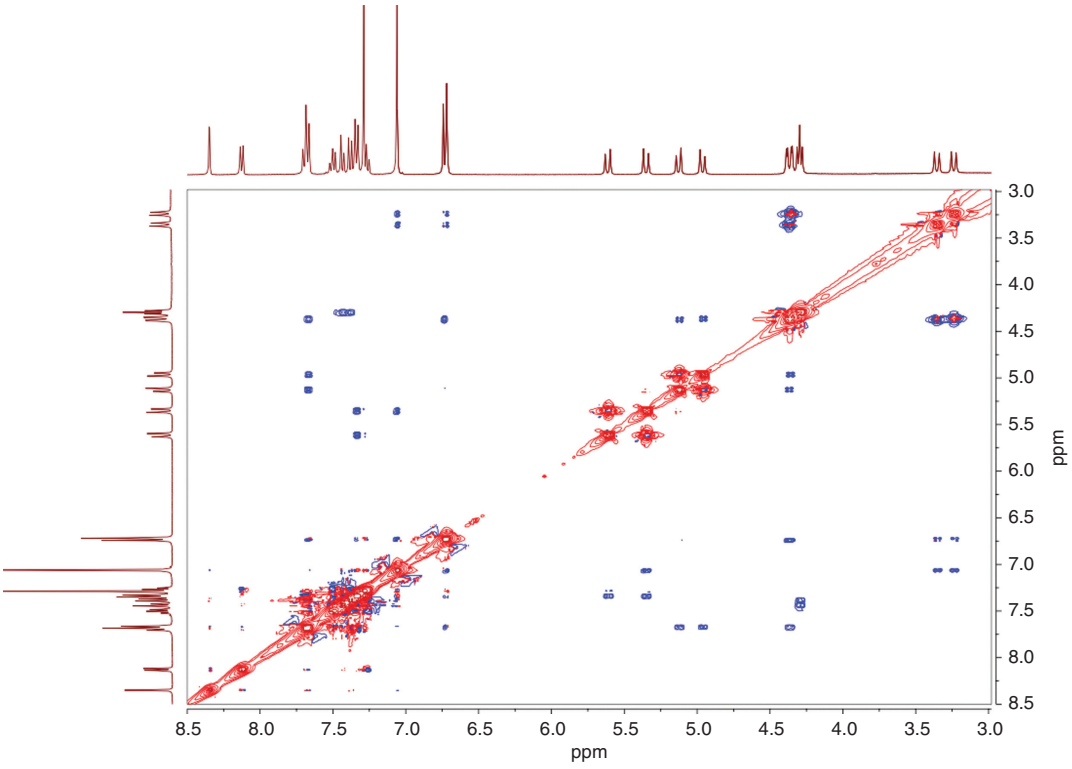

Fig. 2 NOESY spectrum (partial) of *rac*-**2** ($CDCl_3$, 400 MHz, 298 K).

the carbazole moieties, meaning that the oxacyclophane ring introduces a significant rigidity in the whole structures preventing, inter alia, the bending of the CBZ sub-units toward the A rings. This particular feature is noteworthy since it opens the way to the creation of two additional (larger) concave surfaces, electronically and sterically differentiated from the inner cavity of the central calix[4]arene unit, in each side of the plane bisecting the B rings, thus extending the number and the nature of the available binding sites for (chiral) recognition purposes. As will be shown below, these very sites are involved in the recognition events of Pirkle's alcohol. Complementary to the above observation is also the fact that the bridged methylene protons (Ar$CH_{eq}H_{ax}$Ar) appear as two sets of doublets (3.2–3.4 ppm and 4.3–4.4 ppm) and the geminal protons of the benzylene sub-units of the OCP as four well-resolved doublets (4.9–5.6 ppm), definitely showing that **1** and **2** have rigid cone conformations immobilized in C_2-symmetry.

Photophysical properties

Figure 3 depicts the ground-state absorption and steady-state fluorescence spectra of *rac*-**1** and *rac*-**2**. Owing to the different connectivity of the ethynylic linkages in the carbazole sub-units, a higher π-conjugation length is attained in the 2-carbazolyleneethynylene-phenylene-ethynylene-2-carbazolylene chromophore in **1**, resulting in an absorption spectrum slightly red shifted in comparison to 3-carbazolyl isomer **2**. The optical HOMO–LUMO energy gaps (E_g^{opt}), estimated from the low energy onset of the absorption bands of the two compounds, evidence this fact (E_g^{opt} (**1**) = 2.95 eV; E_g^{opt} (**2**) = 3.00 eV).

Although the first transitions in both compounds are fully electric-dipole allowed, a significantly larger ε_{max} (8.0×10^4 $M^{-1}cm^{-1}$) is observed for **1** as compared to **2** ($\varepsilon_{max} = 6.3 \times 10^4$ M^{-1} cm^{-1}). This is related to the higher oscillator strength attained by **1** during the HOMO-LUMO (π–π*) transition, since a larger electric transition dipole moment is generated along the longer molecular axis of the referred chromophore.

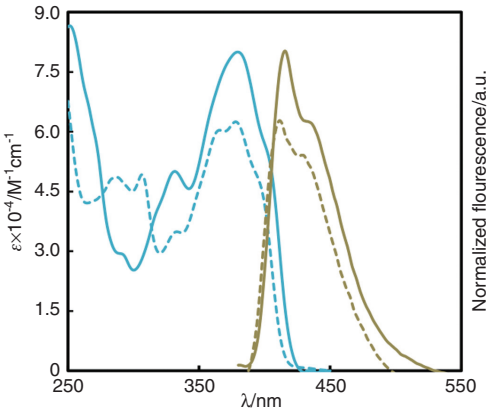

Fig. 3 Absorption and fluorescence spectra of calix[4]arenes **1** (solid line) and **2** (dashed line) in $CHCl_3$ (298 K; λ_{exc} = 380 nm).

The above observations were corroborated by quantum mechanical calculations (B3LYP/6-311G*) [21, 22]. As shown in Fig. 4, the HOMO of **1** extends throughout the entire thread, reaching the remote benzene rings of the carbazole units, whereas in **2** these latter rings are not involved. The computational HOMO–LUMO energy gap is higher for **2** than for **1** by 0.14 eV, in keeping with the experimental E_g^{opt} values.

The bicyclic calix[4]arenes are deep-blue emitters. The fluorescence spectra (Fig. 3) are dominated by 0–0 transitions (λ_{em}^{max} at 416 and 412 nm for **1** and **2**, respectively), with vibronic progressions around 430 nm. As anticipated, both compounds display high fluorescence quantum yields (Φ_F = 0.76 and 0.67 for **1** and **2**, respectively) [23, 24] in fluid phase. Moreover, under conditions of continuous irradiation (λ_{exc} = 380 nm; 298 K), no noticeable photodegradation occurs.

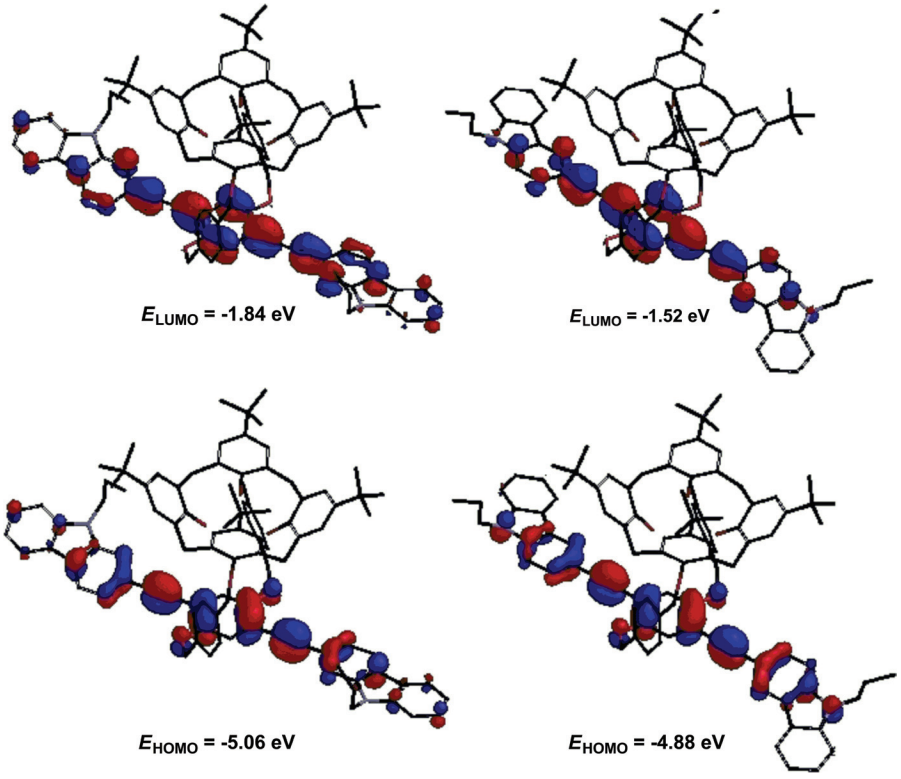

Fig. 4 Plots and energies of the HOMO (bottom) and LUMO (top) of calix[4]arenes **1** (left) and **2** (right) (hydrogens omitted for clarity), depicted on (*pS*) configurations. DFT calculations run at the B3LYP/6-311G* level of theory [21] in vacuo.

Evidence for the inherent chirality, enantiomeric resolution, and chiroptical properties

Calix[4]arenes **1** and **2** are immobilized in C_2-symmetry. Since the rotation of the carbazolyleneethynylene substituents about the *O*-phenylene-*O* axis is precluded by steric reasons, a chirality plane in the quinol moiety of the OCP ring results. The plane of chirality may be defined by the atoms ABXY in the quinol sub-unit, with the pilot atom (Z) located at the benzylic carbon (Fig. 5). The configurational assignment of each enantiomer can then be done by applying the sequence-rule-preferred path [25], as illustrated for calix[4] arene **1** in Fig. 5. Thus, to an observer positioned at Z, the sequence Y→X→B indicates a clockwise rotation and hence a (*pR*) configuration.

^{1}H NMR titration experiments of $CDCl_3$ solutions of **1** and **2** with (*S*)-Pirkle's alcohol [(*S*)-(+)-2,2,2-trifluoro-1-(9-anthryl)ethanol)] provided the first evidence of their chiral nature. Upon addition of up to 5 equiv. of the enantiopure alcohol, the only observable changes were a slight broadening of the signals of **1** and **2**, and a very small but general upfield shift of all resonances, in particular those of the alcohol ($\Delta\delta \sim -0.012$ to -0.026 ppm). On further addition (15 equiv.) however, a definite set of proton signals of **1** and **2** appeared split and doubled, giving a clear indication of the formation of diastereomeric complexes. As illustrated in Fig. 6 for compound **2** (similar changes were observed for **1**), the most characteristic and significant splittings involve several protons of the carbazole sub-unit (CBZ-H_a-H_f), those located on the phenylene (H_e) and on the methylene bridges ($ArCH_{eq}H_{ax}Ar$), as well as some of the benzylic protons ($ArCH_cH_dOAr$). From the location of the observed splittings, it can be concluded that the formation of diastereomeric pairs of **1** and **2** with Pirkle's reagent mainly occurs in the chiral pocket comprehending the calix-OCP *exo* cavities and the carbazole moieties.

While this is a strong evidence of the planar chirality exhibited by **1** and **2**, definitive proof of their enantiomeric nature was obtained from the electronic circular dichroism (CD) spectra of the resolved racemates. The optical resolutions of *rac*-**1** and *rac*-**2** were carried out by chiral HPLC. For the separation, an analytical LiChroCart-(*R*,*R*)-Whelk01 column (250 × 4 mm) was used. After optimization of the separation parameters [26] both antipodes of *rac*-**2** could be nicely separated (Fig. 7). The two isolated fractions (**2**-F_1 and **2**-F_2) could be directly obtained with an enantiomeric excess (ee) of 100 %, with a recover near 50 %. In the case of *rac*-**1**, due to the lower separation and resolution factors [26], while **1**-F_1 was also directly retrieved in 100 % ee, the second eluted fraction was obtained in *ca.* 72 % ee. Its further purification gave **1**-F_2 as an enantiomerically pure sample (Fig. 7).

The CD spectra of the resolved samples (Fig. 8) unequivocally show the enantiomeric relationships of the isolated fractions of **1** and **2**. Absorption and CD spectra of **1** and **2** are composed of several bands due to the various chromophores, including the phenolic and benzylic rings of the calixarene moiety, the carbazole

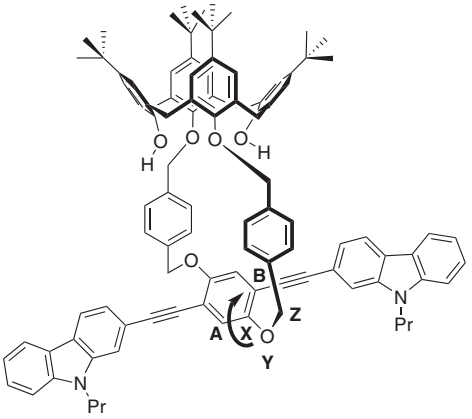

Calix[4]arene (*pR*)-**1**

Fig. 5 Assignment of configuration to ICC **1**.

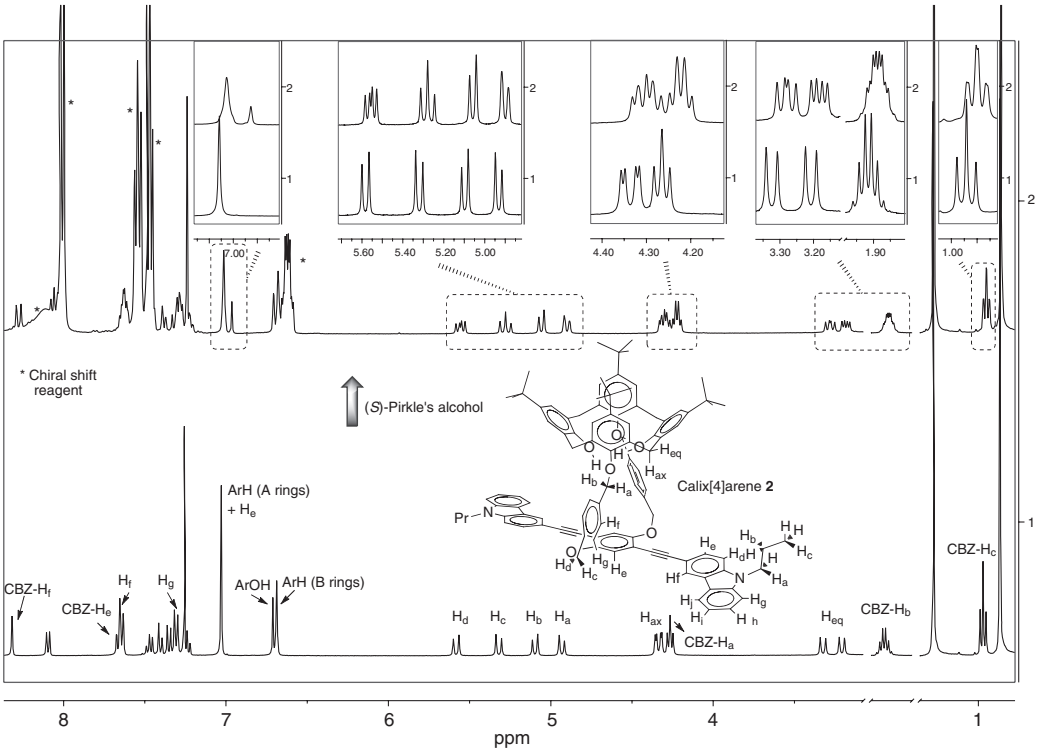

Fig. 6 Representative regions of the ^{1}H NMR spectrum ($CDCl_3$, 400 MHz, 298 K) of **2** (5 mM) (bottom), and those (top) upon addition of (*S*)-Pirkle's alcohol (15 equiv.).

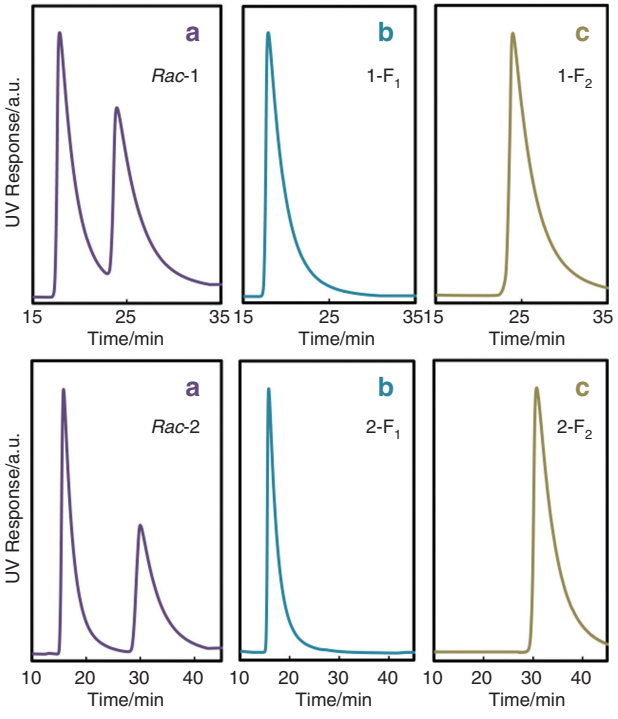

Fig. 7 Enantioresolution of calix[4]arenes **1** (top, a) and **2** (bottom, a). The remaining chromatograms (b and c) correspond to the isolated fractions of each compound. Separation parameters: hexane/propan-2-ol (90:10 (v/v) for **1** and 80:20 for **2**) as eluent at a flow rate of 1 mL/min; UV detection at 350 nm; 298 K).

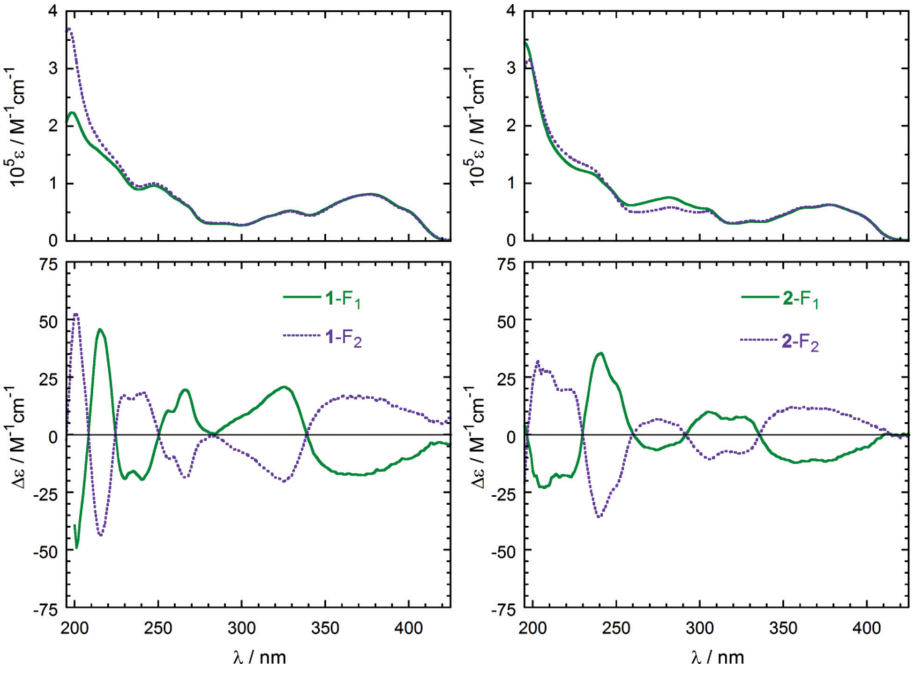

Fig. 8 UV-Vis absorption (top) and CD (bottom) spectra of the enantiomers of **1** (left) and **2** (right), in CH_3CN (6.0×10^{-6} M to 1.0×10^{-5} M at 298 K in 1-cm quartz cells).

rings, and the conjugated phenyleneethynylene unit. This latter, in particular, is the major responsible for the bands above 300 nm. Both compounds **1** and **2** show a bisignate CD spectrum in this region and, in both cases, the first eluted enantiomer F_1 gives a first (longer wavelength) negative and a second positive CD band. We can therefore label the various enantiomers, with reference to the sign of the first CD band, as follows: **1**-F_1 is $(-)_{375}$-**1**; **1**-F_2 is $(+)_{375}$-**1**; **2**-F_1 is $(-)_{375}$-**2**; and **2**-F_2 is $(+)_{375}$-**2**. Below 270 nm, the CD spectra exhibit a series of bands with alternating sign which differ for the two compounds. This is related to the different participation of the CBZ ring to the conjugation of the main chromophore, as discussed above.

In our previous contribution on ICCs [17], we showed that CD calculations with the time-dependent DFT method (TDDFT) [27] offer a way to interpret the observed CD spectra and, most important, to assign the absolute configuration of ICCs. Following the same approach, we considered for each compound a set of structures with (*pS*) configuration, obtained by DFT geometry optimizations [21], with all possible relative

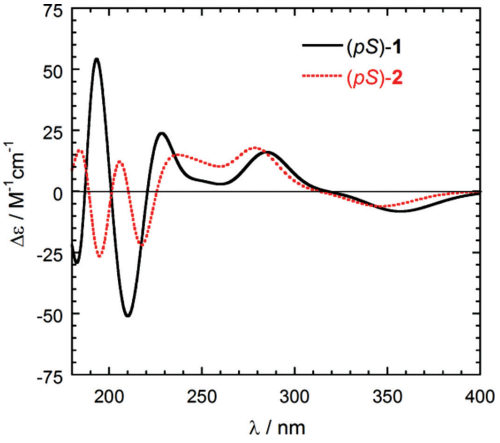

Fig. 9 CD spectra calculated at CAM-B3LYP/SV//B3LYP/6-311G* level in vacuo for (*pS*)-**1** and (*pS*)-**2**. Each spectrum is the arithmetic average of four representative structures (see text); Gaussian band-shape with 0.25 eV exponential half-width.

arrangements of the carbazole units, namely two equivalent *cis* and two distinct *trans* structures [28]. TDDFT calculations were then run at CAM-B3LYP/SV level [29] resulting in the spectra shown in Fig. 9 [30]. Although the agreement with the experimental CD spectra is not perfect, especially for compound **2**, the calculated spectra reproduce several crucial points: a) in the long wavelength region, a bisignate feature is consistently obtained for both compounds; b) in the shorter wavelength region, several bands of alternating sign occur, with marked differences for the two isomers; c) the first CD bands are slightly blue-shifted for isomer **2** with respect to **1**. From the comparison of the calculated and experimental spectra, especially in the long-wavelength region, the enantiomers of **1** and **2** may be assigned the following absolute configurations: for compound **1**, (*pS*)-$(-)_{375}$-**1** is the first eluted (**1**-F_1) and (*pR*)-$(+)_{375}$-**1** the second eluted (**1**-F_2) enantiomer; similarly, for compound **2**, (*pS*)-$(-)_{375}$-**2** is the first eluted (**2**-F_1) and (*pR*)-$(+)_{375}$-**2** the second eluted (**2**-F_2).

In conclusion, following our previously disclosed strategy to ICCs, two new calix[4]arene-based chiral receptors were synthesized using simple procedures. The new fluorescent calix[4]arenes possess rigidified structures and extended recognition sites which altogether may prove useful as a new class of hosts for chirality-mediated events, spanning from chiral sensing to catalysis.

Acknowledgments: We thank Fundação para a Ciência e a Tecnologia/MEC (Portugal) for financial support (PEst-OE/EQB/UI0702/2013 and RECI/QEQ-QIN/0189/2012). G.P. thanks Ministero per l'Istruzione, l'Università e la Ricerca (Italy) for financial support (PRIN2012, prot. 2012A4Z2RY).

References

[1] Z. Asfari, V. Böhmer, J. Harrowfield, J. Vicens (Eds.). *Calixarenes 2001*, Kluwer Academic, Dordrecht (2001).
[2] C. D. Gutsche. "Calixarenes: an introduction". In *Monographs in Supramolecular Chemistry*, 2nd ed., J. F. Stoddart (Ed.), The Royal Society of Chemistry, Cambridge (2008).
[3] A. Casnati, R. Ungaro. In *Calixarenes in Action*, L. Mandolini, R. Ungaro (Eds.), Imperial College Press, London (2000).
[4] A. Arduini, M. Cantoni, E. Graviani, A. Pochini, A. Secchi, A. R. Sicuri, R. Ungaro, M. Vincenti. *Tetrahedron* **51**, 599 (1995).
[5] E. Pinkhassik, I. Stibor, A. Casnati, R. Ungaro. *J. Org. Chem.* **62**, 8654 (1997).
[6] A. Casnati, R. Ungaro. In *Calixarenes in Action*, L. Mandolini, R. Ungaro (Eds.), pp. 62–84, Imperial College Press, London (2000).
[7] P. J. Dijkstra, J. A. J. Brunink, K.-E. Bugge, D. N. Reinhoudt, S. Harkema, R. Ungaro, F Ugozzoli, E. Ghidini. *J. Am. Chem. Soc.* **111**, 7567 (1998).
[8] W. I. I. Bakker, M. Haas, C. Corinne Khoo-Beattie, R. Ostaszewski, S. M. Franken, H. J. den Hertog Jr., W. Verboom, D. de Zeeuw, S. Harkema, D. N. Reinhoudt. *J. Am. Chem. Soc.* **116**, 123 (1994).
[9] C. D. Gutsche, K. A. See. *J. Org. Chem.* **57**, 4527 (1982).
[10] S. Kanamathareddy, C. D. Gutsche. *J. Org. Chem.* **61**, 2511 (1996).
[11] M. J. McIldowie, M. Mocerino, M. I. Ogden. *Supramolecular Chem.* **22**, 13 (2010).
[12] S.-Y. Li, Y.-W. Xu, J.-M. Liu, C.-Y. Su. *Int. J. Mol. Sci.* **12**, 429 (2011).
[13] Y.-S. Zheng, J. Luo. *J. Incl. Phenom. Macrocycl. Chem.* **71**, 35 (2011).
[14] V. Böhmer, D. Kraft, M. Tabatabai. *J. Inclusion Phenom. Mol. Recognit. Chem.* **19**, 17 (1994).
[15] A. D. Cort, L. Mandolini, C. Pasquini, L. Schiaffino. *New J. Chem.* **28**, 1198 (2004).
[16] A. Szumna. *Chem. Soc. Rev.* **39**, 4274 (2010).
[17] J. V. Prata, A. I. Costa, G. Pescitelli, C. M. Teixeira. *Tetrahedron: Asymm.* **25**, 547 (2014).
[18] J. V. Prata, A. I. Costa, C. M. Teixeira. *Tetrahedron Lett.* **54**, 6602 (2013).
[19] P. D. Barata, J. V. Prata. *Supramol. Chem.* **25**, 782 (2013).
[20] Structural assignments of **1** and **2** were based on 2D-NMR spectroscopy techniques (COSY, NOESY, HSCQ and HMBC). Representative ^{1}H NMR (δ/ppm; $CDCl_3$, 400 MHz) data are as follow; for H notations on CBZ sub-unit refer to Fig. 6. Calix[4]arene **1**: 0.87 (s, 18H, C(CH_3)$_3$, B rings), 0.98 (t, *J*=7.3 Hz, 6H, *N*-$CH_2CH_2CH_3$), 1.28 (s, 18H, C(CH_3)$_3$, A rings), 1.85–2.00 (m, 4H, *N*-$CH_2CH_2CH_3$), 3.22 (d, *J*=13.0 Hz, 2H, ArCHH_{eq}Ar), 3.32 (d, *J*=13.3 Hz, 2H, ArCHH_{eq}Ar), 4.27 (t, *J*=7.2 Hz, 4H, *N*-$CH_2CH_2CH_3$), 4.33 (d, *J*=13.2 Hz, 2H, ArCH_{ax}HAr), 4.34 (d, *J*=13.2 Hz, 2H, ArCH_{ax}HAr), 4.93 (d, *J*=12.9 Hz, 2H, Ar_{calix}OC*H*(H)Ar), 5.07 (d, *J*=12.8 Hz, 2H, Ar_{calix}OCH(*H*)Ar), 5.33 (d, *J*=13.9 Hz, 2H, ArC*H*(H)OAr), 5.56 (d, *J*=13.5 Hz, 2H, ArCH(*H*)OAr), 6.66 (s, 2H, ArO*H*), 6.69 (s, 4H, Ar*H*, B rings), 7.04 (s, 4H, Ar*H*, A rings), 7.07 (s, 2H, phenylene), 7.23 (t, *J*=7.4 Hz, 2H, CBZ-H_j), 7.31 (d, *J*=8.0 Hz, 4H, ArH_{meta}(CH_2OAr_{calix}), 7.38-7.50 (m, 6H, CBZ-$H_eH_gH_h$), 7.63 (s, 2H, CBZ-H_d), 7.64 (d, *J*=8.0 Hz, 4H, ArH_{ortho}(CH_2OAr_{calix}); partially overlapped with CBZ-H_d), 8.03 (d, *J*=8.0 Hz, 2H, CBZ-H_i), 8.07 (d, *J*=7.8 Hz, 2H, CBZ-H_j). Anal. Calcd. for $C_{100}H_{100}N_2O_6.2H_2O$: C, 82.16; H, 7.17; N, 1.92. Found: C, 82.05; H, 7.00; N, 2.16. The presence of water was qualitatively confirmed in the ^{1}H

NMR spectrum of similarly dried samples. Calixarene **2**: 0.87 (s, 18H, C(CH_3)$_3$, B rings), 0.97 (t, *J*=7.4 Hz, 6H, *N*-$CH_2CH_2CH_3$), 1.28 (s, 18H, C(CH_3)$_3$, A rings), 1.85-2.00 (m, 4H, *N*-$CH_2CH_2CH_3$), 3.21 (d, *J*=13.0 Hz, 2H, ArCHH_{eq}Ar), 3.32 (d, *J*=13.3 Hz, 2H, ArCHH_{eq}Ar), 4.27 (t, *J*=7.1 Hz, 4H, *N*-$CH_2CH_2CH_3$), 4.33 (d, *J*=13.2 Hz, 2H, ArCH_{ax}HAr), 4.34 (d, *J*=13.2 Hz, 2H, ArCH_{ax}HAr), 4.93 (d, *J*=12.8 Hz, 2H, Ar_{calix}OC*H*(H)Ar), 5.10 (d, *J*=12.8 Hz, 2H, Ar_{calix}OCH(*H*)Ar), 5.32 (d, *J*=13.8 Hz, 2H, ArC*H*(H)OAr), 5.58 (d, *J*=13.8 Hz, 2H, ArCH(*H*)OAr), 6.69 (s, 4H, Ar*H*, B rings), 6.71 (s, 2H, ArO*H*), 7.03 (s, 4H, Ar*H*, A rings and s, 2H, phenylene; accidental isochrony), 7.21-7.27 (m, 2H, CBZ-H_i; partially overlapped with $CHCl_3$), 7.31 (d, *J*=8.0 Hz, 4H, ArH_{meta}(CH_2OAr_{calix}), 7.35 (d, *J*=8.5 Hz, 2H, CBZ-H_d), 7.40 (d, *J*=8.1 Hz, 2H, CBZ-H_g), 7.44-7.50 (m, 2H, CBZ-H_h), 7.64 (d, *J*=8.0 Hz, 4H, ArH_{ortho}(CH_2OAr_{calix}); partially overlapped with CBZ-H_e), 7.64-7.69 (m, 2H, CBZ-H_e), 8.10 (d, *J*=7.7 Hz, 2H, CBZ-H_j), 8.32 (d, *J*=1.0 Hz, 2H, CBZ-H_f). Anal. Calcd. for $C_{100}H_{100}N_2O_6.H_2O$: C, 83.18; H, 7.12; N, 1.94. Found: C, 83.35; H, 7.22; N, 2.18. The presence of water was qualitatively confirmed in the ^{1}H NMR spectrum of similarly dried samples.

[21] Conformational searches (Monte Carlo method, MMFF force field) were first performed on (*pS*) configurations of **1** and **2**, which were followed by geometry optimizations (AM1 semi-empirical model) of the lowest-energy conformers; single-point energy calculations were then run with a hybrid density functional model (B3LYP) using 6-311G* basis sets, as developed in Spartan'04 [22]. The input structures for CD calculations were optimized at B3LYP/6-31G* level.

[22] Spartan'04 Molecular Modeling Program, Wavefunction, Inc., Irvine, CA, 2005.

[23] The fluorescence quantum yields of **1** and **2** in $CHCl_3$ were determined [24] using 9,10-diphenylanthracene as reference (Φ_F = 0.72, ethanol) in air-equilibrated conditions (λ_{exc} = 380 nm; right angle geometry in 1-cm quartz cells); the optical densities of the samples and reference were kept below 0.05 at the excitation wavelength to prevent inner filter effects.

[24] D. F. Eaton. *Pure Appl. Chem.* **60**, 1107 (1988).

[25] B. Testa. *Helv. Chim. Acta* **96**, 351 (2013).

[26] Under the here reported conditions, and using 1,2,3-trimethylbenzene as the void volume marker, the separation (α) and the resolution (R_s) factors [17] were calculated. For *rac*-**1**, α = 1.41 and R_s = 2.66, and for *rac*-**2**, α = 2.04 and R_s = 4.45.

[27] J. Autschbach, L. Nitsch-Velasquez, M. Rudolph. *Top. Curr. Chem.* **298**, 1 (2011).

[28] With *cis* and *trans* we indicate that the nitrogen atoms of the carbazoles are oriented toward the same or opposite directions respectively. In all cases, the carbazolyleneethynylene-phenylene-ethynylenecarbazolylene units were almost coplanar. In practice, however, there is an almost free rotation around the ethynylic linkages. Taking this aspect into account would be very computationally demanding (see discussion in ref [17]) and would not reverse the configurational assignment.

[29] DFT and TDDFT calculations were run with Gaussian09 (Revision D.01, Gaussian, Inc., Wallingford CT, 2009) using default grids and convergence criteria. The references for the employed functionals and basis sets may be found online at http://www.gaussian.com/g_tech/g_ur/l_keywords09.htm.

[30] Since the four structures considered for each compound do not represent a true conformational ensemble [28], calculated spectra were simply averaged and not weighted on the basis of relative energies.